

Optical properties of the Ce and La ditelluride charge density wave compounds

M. Lavagnini, A. Sacchetti, and L. Degiorgi

Laboratorium für Festkörperphysik, ETH-Zürich, CH-8093 Zürich, Switzerland

K. Y. Shin and I. R. Fisher

Geballe Laboratory for Advanced Materials and Department of Applied Physics, Stanford University, Stanford, California 94305-4045, USA

(Received 19 January 2007; revised manuscript received 28 March 2007; published 31 May 2007)

The La and Ce ditellurides LaTe_2 and CeTe_2 are deep in the charge-density-wave (CDW) ground state even at 300 K. We have collected their electrodynamic response over a broad spectral range from the far infrared up to the ultraviolet. We establish the energy scale of the single particle excitation across the CDW gap. Moreover, we find that the CDW collective state gaps a large portion of the Fermi surface. Based on the observation of a power-law behavior in the optical conductivity, similar to that found for the related rare-earth tritellurides but over a reduced frequency range, we suggest that interactions and umklapp processes may play a role in the onset of the CDW broken-symmetry ground state.

DOI: [10.1103/PhysRevB.75.205133](https://doi.org/10.1103/PhysRevB.75.205133)

PACS number(s): 71.45.Lr, 78.20.-e

I. INTRODUCTION

Charge-density wave (CDW) is a paramount example of broken-symmetry ground state principally driven by the electron-phonon interaction and occurring in low-dimensional materials. More than 50 years ago, Peierls first pointed out that a one-dimensional (1D) metal coupled to the underlying lattice is indeed not stable at low temperatures.¹ In most cases, the instability in one dimension leads to a metal-insulator phase transition. The excitation spectrum of the resulting ground state of such a coupled electron-phonon system is characterized by a gap absorption feature, as a consequence of the Fermi surface (FS) nesting with wave vector $q=2k_F$, and by a collective mode formed by electron-hole pairs at $q=2k_F$.² In contrast to superconductors, the phase excitations of the collective mode are gapless. Consequently, electrostatic potentials (due to impurities, grain boundaries, surface effect, etc.) break the translational symmetry and lead to the pinning of the collective mode. This ultimately results in a nonconducting but highly polarizable ground state in one dimension.² By increasing the dimensionality of the interacting electron gas system, the impact of the nesting is less relevant and the fraction of gapped FS is reduced. CDW transitions then lead, in two dimensions, to a pseudogap feature in the density of states and those two-dimensional (2D) systems remain metallic down to low temperatures. That increasing the dimensionality less affects the FS is also well represented by the progressive suppression of the singularity in the Lindhard response function at $q=2k_F$, which, in fact, totally disappears in three dimensions.² Furthermore, low dimensionality has a strong impact on the normal-state properties, as well, which particularly in one dimension can be suitably explained within the Tomonaga-Luttinger liquid or Luther-Emery scenarios.^{3,4}

The formation of CDW ground states is, by now, well documented in a broad range of low-dimensional solids,² among which we encounter the linear-chain organic and inorganic compounds. An effective low dimensionality has also been identified in the layered $R\text{Te}_2$ ($R=\text{La}$ and Ce), which play host to a CDW state, described in terms of modu-

lated Cu_2Sb -type structure (Pa/nmm) based on alternating layers of square-planar Te sheets and a corrugated $R\text{Te}$ slab.^{5,6} It is worth noting that no clear electronic phase transitions are observed below 300 K, and the material appears to be deep in the CDW state even at room temperature. A substantial anisotropy in the electrical resistivity along different crystallographic directions confirms the quasi-2D character of the charge carriers. The resistivity ratio (ρ_c/ρ_{ab}) between the c axis and the ab plane at low temperatures is about 50 for the La and 100 for the Ce compound.⁵ The temperature dependence of the resistivity is reminiscent of either a doped small-gap semiconductor or possibly a semi-metal, and is certainly far from that of a good metal. Long-range magnetic order of the local $4f$ electrons in CeTe_2 leads to an additional feature in the resistivity at $T_N \sim 6$ K. This temperature is far below the energy scale associated with the CDW and for the purposes of this discussion can be safely ignored.⁵ A superlattice modulation of the average structure has been observed via transmission electron microscopy^{5,7} and x-ray diffraction,⁸ with somewhat different modulation wave vectors for the two compounds. Tunneling experiment⁹ and angle-resolved photoemission spectroscopy (ARPES) reveal a large CDW gap (the ARPES gap^{5,6,10} extends between 100 and 600 meV). Regions with the larger gap (~ 600 meV) imply strong coupling, while those with smaller gap (~ 100 meV) seem to be characterized by imperfect nesting, making the position of the small-gap regions very sensitive to details of the CDW condensate.⁵ The gap was found to vary in magnitude around the FS rather differently for the two compounds,^{5,6} presumably reflecting the different lattice modulations. Since the title compounds are essentially quasi-2D materials, the FS is only partially gapped by the CDW transition, so that ungapped charge carriers contribute to the conductivity at low temperatures. Heat-capacity measurements at low temperatures also indicate a very small electronic density of states, consistent with the measured electrical resistivity.⁵ All of these experimental observations essentially establish the lattice modulation in $R\text{Te}_2$ as a CDW, driven by an electronic instability of the FS.

$R\text{Te}_2$ share several common features and similar properties with the related bilayer $R\text{Te}_3$ materials.¹¹ Nonetheless, there are also important differences. First of all, the calculated Lindhard susceptibility $\chi(q)$ does not have a simple single peak but rather has a tendency to have a range of maxima corresponding to nesting of different regions of the Fermi surface. In contrast, similar calculations for $R\text{Te}_3$ reveal a very well-defined maximum in $\chi(q)$.⁵ One consequence of this difference between $R\text{Te}_2$ and $R\text{Te}_3$ is that the lattice modulation is somewhat different for each member of the ditelluride family of compounds but is essentially identical for all members of the tritelluride family, being characterized in that case by a simple unidirectional wave vector. An additional difference between these two families of compounds lies in their widths of formation. Whereas $R\text{Te}_3$ appears to be a line compound, $R\text{Te}_2$ is known to have a substantial width of formation. As a consequence, while single crystals of $R\text{Te}_3$ do not exhibit sample-to-sample variation, there is an appreciable variation in the resistivity of single crystals of $R\text{Te}_2$ even when taken from the same growth batch. Variation in the Te concentration for different members of the rare-earth ditellurides makes a systematic study across the whole rare-earth series in $R\text{Te}_2$ somewhat less meaningful than has been the case for the rare-earth tritellurides. Nevertheless, comparison of the data for $\text{CeTe}_{2.00}$ and $\text{LaTe}_{1.95}$ with similar data for $R\text{Te}_3$ does enable us to make some general observations about the similarities and differences between these two closely related families of compounds.

The structural and electronic simplicity of $R\text{Te}_2$ and $R\text{Te}_3$, combined with the large size of the CDW gap, makes these materials particularly attractive for studying the effect of CDW formation on the electronic structure of layered systems. One approach is to exploit optical spectroscopy methods, which are ideal experimental tools to get insight into the absorption spectrum of the investigated materials. Optical data allow, in principle, to address both the gapped as well as the ungapped fractions of FS.¹¹ The measurements for these particularly well-studied members of the rare-earth ditellurides series were also partially inspired by the desire to reconcile ARPES results (which show ungapped sections^{5,6,10} of FS) with dc resistivity measurements (which are not characteristics of a good metal⁵). Furthermore, the frequency dependence of the absorption spectrum will shed light on the possible non-Fermi liquid nature of the electronic properties of these low-dimensional layered compounds.

II. EXPERIMENT AND RESULTS

We report a comprehensive optical study on LaTe_2 and CeTe_2 single crystals, which were grown in this case by slow cooling a binary melt, as described previously in Ref. 5. Samples grown by this technique are as close to stoichiometric as possible, having compositions $\text{CeTe}_{2.00}$ and $\text{LaTe}_{1.95}$ as determined by electron microprobe analysis using elemental standards, with an uncertainty of ± 0.03 in the Te content. Detailed characterization of these samples can be found in Ref. 5. The crystals were polished in order to achieve a clean surface for the reflectivity measurements.

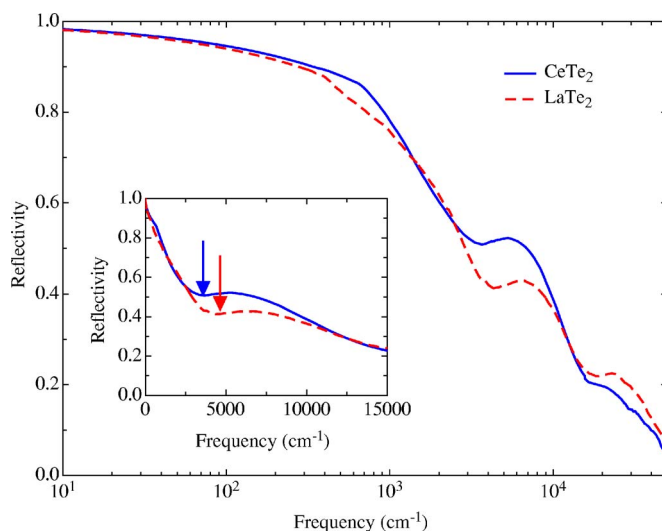


FIG. 1. (Color online) $R(\omega)$ of LaTe_2 and CeTe_2 at 300 K. The inset is a blow-up of $R(\omega)$ emphasizing the broad absorption feature in the midinfrared spectral range. The arrows mark the shallow minimum in $R(\omega)$ at the onset of the broad absorption, peaked between 5000 and 6000 cm^{-1} and overlapped to the plasma edge feature.

Exploiting several spectrometers and interferometers, the optical reflectivity $R(\omega)$ was measured for all samples from the far-infrared (6 meV) up to the ultraviolet (6 eV) spectral range, with light polarized parallel to the Te planes. Details pertaining to the experiments can be found elsewhere.¹¹⁻¹³

Figure 1 displays $R(\omega)$ for both title compounds over the whole investigated spectral range. $R(\omega)$ does not display any temperature dependence between 300 and 10 K in the covered energy interval and merges to total reflection for frequency going to zero for both compounds. The $R(\omega)$ spectra are therefore typical of an overall metallic behavior. Overlapped to the plasma edge feature (for $\omega < 10^4 \text{ cm}^{-1}$), one can observe, furthermore, a rather broad absorption centered at about 6000 cm^{-1} . This feature is emphasized by the blow-up of $R(\omega)$ (inset in Fig. 1).

These characteristic fingerprints of the electrodynamic response in $R\text{Te}_2$ are even better highlighted in the real part $\sigma_1(\omega)$ of the optical conductivity, shown in Fig. 2. $\sigma_1(\omega)$ is achieved through standard Kramers-Kronig transformation^{12,13} of $R(\omega)$. To this purpose, $R(\omega)$ was extended toward zero frequency (i.e., $\omega \rightarrow 0$) with the Hagen-Rubens extrapolation $R(\omega) = 1 - 2\sqrt{\omega/\sigma_{dc}}$ and with standard power-law extrapolations at high frequencies (i.e., $\omega > 5 \times 10^4 \text{ cm}^{-1}$). The dc conductivity values employed in the Hagen-Rubens extension of $R(\omega)$ are in fair agreement with transport measurements.⁵ In $\sigma_1(\omega)$ we observe the so-called effective Drude resonance below 1000 cm^{-1} , due to the free charge carriers, and the midinfrared absorption at 5000 and 6000 cm^{-1} for CeTe_2 and LaTe_2 (arrows in Fig. 2), respectively, which will be ascribed later to the single-particle excitation across the CDW gap. At higher frequencies, there is also a broad feature centered at about $2 \times 10^4 \text{ cm}^{-1}$ signaling the onset of electronic interband transitions. Tight-binding band-structure calculations reveal, indeed, the presence of ex-

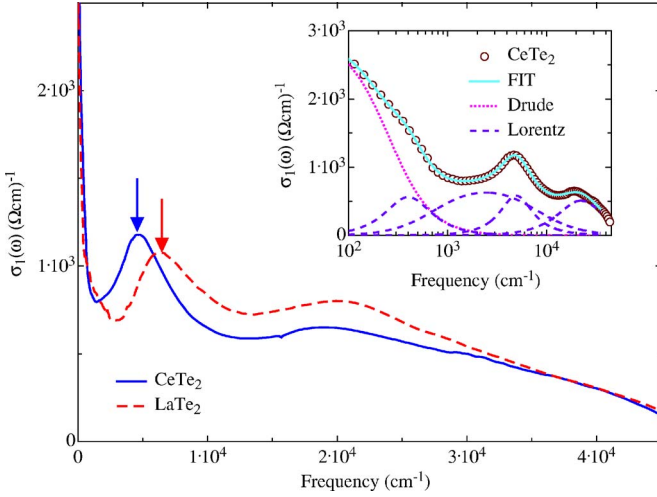


FIG. 2. (Color online) Room temperature $\sigma_1(\omega)$ of LaTe_2 and CeTe_2 . Arrows mark the position of the midinfrared peak for each compound (see text). Inset: Drude-Lorentz fit for CeTe_2 , showing the experimental data, the total fitted curve, and the Drude-Lorentz components.

citations due to the electronic interband transitions well above 1 eV.^{5,14}

In order to facilitate the discussion and to better identify the characteristic features in the electrodynamic response of these rare-earth ditellurides, we describe their absorption spectrum within the Lorentz-Drude phenomenological approach.^{12,13} It consists in reproducing the dielectric function by the following expression:

$$\tilde{\epsilon}(\omega) = \epsilon_1(\omega) + i\epsilon_2(\omega) = \epsilon_\infty - \frac{\omega_p^2}{\omega^2 + i\omega\gamma_D} + \sum_j \frac{S_j^2}{\omega^2 - \omega_j^2 - i\omega\gamma_j}, \quad (1)$$

where ϵ_∞ is the optical dielectric constant, ω_p and γ_D are the plasma frequency and the width of the Drude peak, respectively, whereas ω_j , γ_j , and S_j^2 are the center-peak frequency, the width, and the mode strength for the j th Lorentz harmonic oscillator (ho), respectively. $\sigma_1(\omega)$ is then obtained from $\sigma_1(\omega) = \omega\epsilon_2(\omega)/4\pi$.

The fits of all spectra were extended up to $4 \times 10^4 \text{ cm}^{-1}$. Besides the Drude contribution, four Lorentz ho's for each compound are required to fit all features at finite frequencies. The three lowest frequency ho's will be associated below with the CDW gap excitation, while the fourth one will rep-

resent the first excitation at the onset of the high-frequency electronic transitions. This is explicitly shown in the inset of Fig. 2 for the Ce compound, where the fit components are displayed together with the total fit. The fit quality is astonishingly good for both investigated compounds.

III. DISCUSSION

The depletion in the $\sigma_1(\omega)$ spectrum (Fig. 2) between the Drude component and the absorption feature at about 6000 cm^{-1} bears a rather striking similarity with the situation encountered in the absorption spectrum of the bilayer RTe_3 .¹¹ Making use of the analogous notation of Ref. 11, the depletion in $\sigma_1(\omega)$ identifies the onset for the excitation across the CDW gap into the single particle (SP) states, giving rise to the midinfrared absorption. From now on we will refer to this midinfrared absorption as SP peak. We note from Fig. 2 and its inset that the SP peak coincides with the third Lorentz ho at about 5000 and 6000 cm^{-1} for CeTe_2 and LaTe_2 , respectively. Nonetheless, this SP absorption feature is also characterized by a rather broad low-frequency tail (represented in the fit by the two lowest ho's), which extends well within the high-frequency tail of the Drude component. This might indicate, on the one hand, that the metallic component is not simply Drude-like and that some localization occurs or, on the other hand, that the SP peak in each compound can be thought of as composed of the superposition of several excitations. These latter excitations, in analogy to RTe_3 ,¹¹ would mimic a continuous distribution of gap values, as seen in ARPES.^{5,6} This would also mean that the CDW gap differently affects the FS, with perfectly nested regions of FS with a large gap and nonperfectly nested ones with a small gap.

Following our previous work on RTe_3 (Ref. 11) and tending towards the scenario in which the data are described by a distribution of gaps as suggested by ARPES measurements,⁵ we can similarly introduce a so-called averaged quantity ω_{SP} :

$$\omega_{SP} = \frac{\sum_{j=1}^3 \omega_j S_j^2}{\sum_{j=1}^3 S_j^2}, \quad (2)$$

which represents the center of mass of the SP excitation. Here ω_{SP} provides an average single energy scale, estimating the optical CDW gap. Table I displays the values of ω_{SP} for both compounds. ω_{SP} for the rare-earth ditellurides decreases

TABLE I. The first two columns summarize the values ω_p and ω_{SP} [Eq. (2)], both in cm^{-1} . The third column reports the ratio Φ between the Drude spectral weights (see text) in the CDW and normal states. The last four columns report the effective mass m_{NS} and carrier density n_{NS} in the normal state and effective mass m_{CDW} and carrier density n_{CDW} in the CDW state for both samples. Carrier densities and effective masses are given in carriers/cell and m_e units, respectively.

Samples	ω_p	ω_{SP}	Φ	m_{NS}	n_{NS}	m_{CDW}	n_{CDW}
LaTe_2	6840	5502	0.0845	1.2	1.3	0.3	0.03
CeTe_2	6658	3165	0.0805	1.2	1.4	0.3	0.03

by almost a factor of 2 going from LaTe₂ to CeTe₂, while it was almost identical between CeTe₃ and LaTe₃. ω_{SP} in LaTe₂ is comparable to the value for LaTe₃ and in CeTe₂ is smaller than in CeTe₃.¹¹ Our gap values in RTe₂ lie in the interval of CDW gaps, estimated from ARPES data.^{5,6}

The spectral weight encountered in the Drude component is also of interest: the plasma frequency ω_p in the CDW state remains almost constant (Table I) in the La and Ce ditellurides, while it slightly increases from LaTe₃ to CeTe₃. ω_p obviously refers to the ungapped fraction of FS, thus responsible for the effective metallic behavior even within the CDW phase. For these ungapped carriers in the CDW state, we assume a 2D free-hole scenario. The Sommerfeld γ value of the specific heat and the charge-carrier effective mass m_{CDW} in the CDW phase are related by¹¹

$$\gamma = \frac{\pi k_B^2 m_{CDW} a^2}{3 \hbar^2}. \quad (3)$$

Using $\gamma = 0.0003$ J/mol K² for LaTe₂,^{5,15} we achieve m_{CDW} for both compounds, as reported in Table I. m_{CDW} for RTe₂ is significantly smaller than in RTe₃.¹¹ This would already anticipate that the CDW condensate and the related nesting of the Fermi surface in RTe₂ mainly gap states, which are much closer to the band edge and with smaller band curvature than in RTe₃. We can now exploit ω_p in order to obtain the free charge-carrier concentration in the CDW state, listed in Table I, as well.

It is worth extending this analysis to the hypothetical normal state (NS), which should develop at temperatures much higher than 300 K. Again we make use of our previous analysis for the rare-earth tritellurides¹¹ and we exploit an elementary 2D tight-binding calculation involving the Te p_x and p_y orbitals.⁵ The Fermi energy, associated to the holelike charge carriers, is $E_F = 1.95$ eV. Therefore, considering a parabolic expansion of the 2D bands around their maximum, E_F is then related to the effective mass m_{NS} in the (hypothetical) NS by¹¹

$$E_F = \frac{\pi \hbar^2 n_{2D}}{m_{NS}}, \quad (4)$$

where n_{2D} is the 2D hole density in NS. With $n_{2D} = 2/a^2$ ($a = 4.5$ Å, for both compounds¹⁶), the resulting m_{NS} are reported in Table I. m_{CDW} and m_{NS} describe the average curvature of the free charge-carrier bands in CDW and NS, respectively. There is approximately a factor of 4 between m_{NS} and m_{CDW} (in the RTe₃ compounds, it was a factor¹¹ of 2). Such a difference suggests again that in the CDW phase the average curvature of the bands is larger than in NS.

The m_{NS} values allow us to extract the NS charge-carrier concentration n_{NS} , which can then be directly compared with n_{ch} , estimated from the chemical counting.⁶ Prerequisite for the achievement of n_{NS} is, first of all, the estimation of the total spectral weight associated with the itinerant charge carriers in NS. If we assume the conservation of the spectral weight between the CDW and the normal state, and that there will be no SP peak in the (hypothetical) NS, the Drude contribution in NS would then have a total spectral weight given by $S_{NS}^2 = \omega_p^2 + \sum_{j=1}^3 S_j^2$.¹¹ Therefore, from $S_{NS}^2 \sim n_{NS}/m_{NS}$

we obtain n_{NS} as reported in Table I. The n_{NS} values are indeed very close to $n_{ch} = 2$.¹⁷ While differences in the stoichiometry of the two compounds due to Te vacancies might account for a small part of this difference, the origin of the discrepancy most likely lies in the approximations we have used to extract n_{NS} . Given the experimental uncertainties, the rather fair agreement between n_{NS} and n_{ch} adds confidence to the reliability of our analysis.

From our data, we can also estimate the quantity $\Phi = \omega_p^2 / (\omega_p^2 + \sum_{j=1}^3 S_j^2)$ (Table I), representing the ratio between the spectral weight of the Drude peak and the total spectral weight of the Drude term and midinfrared absorption. Φ roughly measures, as previously described in Ref. 11, the fraction of the ungapped FS area (i.e., those parts of FS which are not affected by the CDW state). The very small values of Φ confirm that a large portion of FS for both La and Ce ditellurides is gapped. Large gapped regions of FS has also been evidenced from recent ARPES data, although the relative ratio of the gapped regions was found to be rather different for the two compounds.⁵ Φ in RTe₂ is slightly larger than in RTe₃, indicating that the nesting is more efficient in the rare-earth tritellurides. Nevertheless, the presence of only a very small number of carriers at the Fermi energy of RTe₂ could be one reason for the bad metallicity observed by electrical conductivity as well as heat capacity.⁵ In contrast, RTe₃ is found to have much better metallic properties and a larger electronic contribution to the heat capacity than RTe₂. This is not inconsistent with $\Phi_{RTe_3} < \Phi_{RTe_2}$, owing to the different size of FS in these two materials. We also note that there is a substantial disorder in the La compound arising from the Te vacancies, an effect all but absent in the stoichiometric tritelluride compounds. Therefore, polaronic and/or localization effects may also play a significant role in substantially reducing the conductivity and giving origin to the bad metallicity of these compounds.

We have also observed a power-law behavior [$\sigma_1(\omega) \sim \omega^\eta$] in RTe₂ for frequencies above ω_{SP} . This is shown in Fig. 3 for both investigated compounds, using a scaled representation. η for RTe₂ ranges between -0.7 and -1 for the La and Ce compounds, respectively. While these η values compare rather well with those in RTe₃, the power-law behavior only extends over a much smaller spectral range than in RTe₃.¹¹ Previously, we argued that for RTe₃ an exponent η of the order of -1 is the consequence of direct interaction between electrons, as source for umklapp scattering.¹⁸ Although the evidence is less clear-cut for LaTe₂ and CeTe₂ due to the limited range of frequencies before the trend is obscured by additional interband transitions, nevertheless, it seems likely that a similar effect is present in these materials. At least at high-energy scales, there is then evidence of a typical Tomonaga-Luttinger liquid scenario, emphasizing a non-negligible contribution of 1D correlation effects in the physics of these 2D compounds.^{4,11,18} In such a case, a standard electron-phonon mechanism in RTe₂, as in RTe₃, may not be enough to fully account for the CDW formation, although further experiments will be necessary to firmly establish this hypothesis.

IV. CONCLUSIONS

In summary, we have described the optical response in RTe₂ for $R = \text{La}$ and Ce . Our data, besides revealing the *SP*

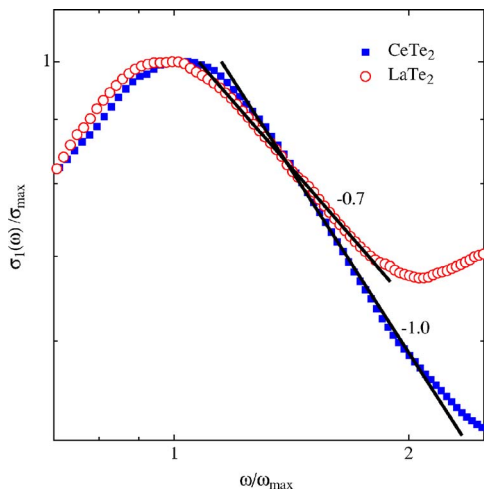


FIG. 3. (Color online) $\sigma_1(\omega)$ of $R\text{Te}_2$ ($R=\text{La}$ and Ce) plotted on a bilogarithmic scale. The y axis is scaled by the maximum of the midinfrared peak in σ_1 , while the energy axis is scaled by the frequency where the maximum in $\sigma_1(\omega)$ occurs. The solid lines are power-law fits to the data (the exponents are given in the figure).

excitation across the CDW gap, also indicate that a large portion of FS is gapped for both compounds. Our data show that the materials are bad metal, lending weight to the ARPES results, and illustrate some rather important differences to the tritellurides (for instance, a significantly reduced inertia of the itinerant charge carriers in the CDW state of $R\text{Te}_2$). At the same time, our findings suggest that there are

also some intriguing similarities between the two families of compounds—not least of which is the power-law behavior at high frequencies.

ARPES and thermodynamic experiments have pointed out the sensitive role played by perturbation, like Te vacancies, on the CDW state.⁵ Such a sensitivity is even stronger than in $R\text{Te}_3$ and it has been mainly associated with the observation that the nesting wave vectors, particularly in CeTe_2 , are somewhat poorly defined.⁵ Besides the Te deficiencies, changes in the rare earth (chemical pressure) may also lead to subtle differences in the lattice modulation. Therefore, applied pressure might also affect to some extent the electronic structure and the CDW condensate and might therefore be used to differentiate between the effects of chemical pressure and vacancy concentration in determining the differences between these two compounds. Analogous to $R\text{Te}_3$,¹⁹ pressure-dependent optical investigations may be of great relevance. Such investigations are in progress and will be reported elsewhere.

ACKNOWLEDGMENTS

The authors wish to thank J. Müller for technical help and V. Brouet for fruitful discussions. One of us (A.S.) wishes to acknowledge financial support from the Della Riccia Foundation. This work has been supported by the Swiss National Foundation for the Scientific Research within the NCCR MaNEP pool. This work is also supported by the Department of Energy, Office of Basic Energy Sciences under Contract No. DE-AC02-76SF00515.

¹R. Peierls, *Quantum Theory of Solids* (Clarendon, Oxford, 1955).

²G. Grüner, *Density Waves in Solids* (Addison-Wesley, Reading, MA, 1994).

³*Strong Interactions in Low Dimensions*, edited by D. Baeriswyl and L. Degiorgi (Kluwer Academic, Dordrecht, 2004).

⁴V. Vescoli, F. Zwick, W. Henderson, L. Degiorgi, M. Grioni, G. Gruner, and L. K. Montgomery, *Eur. Phys. J. B* **13**, 503 (2000).

⁵K. Y. Shin, V. Brouet, N. Ru, Z. X. Shen, and I. R. Fisher, *Phys. Rev. B* **72**, 085132 (2005), and references therein.

⁶J.-S. Kang, C. G. Olson, Y. S. Kwon, J. H. Shim, and B. I. Min, *Phys. Rev. B* **74**, 085115 (2006).

⁷E. DiMasi, B. Foran, M. C. Aronson, and S. Lee, *Phys. Rev. B* **54**, 13587 (1996).

⁸K. Stöwe, *J. Solid State Chem.* **149**, 155 (2000); *J. Alloys Compd.* **307**, 101 (2000).

⁹M. H. Jung, T. Ekino, Y. S. Kwon, and T. Takabatake, *Phys. Rev. B* **63**, 035101 (2000).

¹⁰The gap values determined from the ARPES experiments are always referred with respect to the Fermi energy. Assuming the Fermi energy in the middle of the gap, means that the optically determined gap is about twice as large as the ARPES one.

¹¹A. Sacchetti, L. Degiorgi, T. Giamarchi, N. Ru, and I. R. Fisher, *Phys. Rev. B* **74**, 125115 (2006), and references therein.

¹²M. Dressel and G. Grüner, *Electrodynamics of Solids* (Cambridge University Press, Cambridge, 2002).

¹³F. Wooten, *Optical Properties of Solids* (Academic, New York,

1972).

¹⁴J. Laverock, S. B. Dugdale, Zs. Major, M. A. Alam, N. Ru, I. R. Fisher, G. Santi, and E. Bruno, *Phys. Rev. B* **71**, 085114 (2005).

¹⁵Analogous to $R\text{Te}_3$ (Ref. 11), we use the γ value of LaTe_2 for CeTe_2 , as well. For magnetic members of the rare-earth series it is difficult to extract γ from thermodynamic experiments. However, since the chemical and structural changes are small and even though the modulation wave vectors and density of states at E_F are rather different among the two compounds (Refs. 5 and 6), the assumption of equal γ for both compounds seems to be a reasonable approximation at this point.

¹⁶P. Villars and L. D. Calvert, *Pearson's Handbook of Crystallographic Data for Intermetallic Phases* (American Society for Metals, Metals Park, OH, 1991).

¹⁷The ionic configuration of $R\text{Te}_2$ is considered to be $R^{3+}\text{Te}(2)^{2-}\text{Te}(1)^{1-}$ so as to produce hole carriers in the $\text{Te}(1)$ sheets, precisely one hole for each formula unit. Since the unit cell contains 2 f.u., the number of the hole carriers (n_{ch}) inside the unit cell is 2, same as the number of $\text{Te}(1)^{1-}$ atoms in the planar sheets (Ref. 6). We note that n_{ch} corresponds to a 3/4 full band since the p_z orbitals are filled.

¹⁸T. Giamarchi, *Quantum Physics in One Dimension* (Oxford University Press, Oxford, 2004).

¹⁹A. Sacchetti, E. Arcangeletti, A. Perucchi, L. Baldassarre, P. Postorino, S. Lupi, N. Ru, I. R. Fisher, and L. Degiorgi, *Phys. Rev. Lett.* **98**, 026401 (2007).